Proceedings of the Seventeenth International Conference on
Civil, Structural and Environmental Engineering Computing
Edited by: P. Iványi, J. Kruis and B.H.V. Topping
Civil-Comp Conferences, Volume 6, Paper 12.2
Civil-Comp Press, Edinburgh, United Kingdom, 2023
doi: 10.4203/ccc.6.12.2

Seismic Response of Tunnel-group Metro Station in a Rock Site

R. Li[1] and Y. Yuan[1,2]

[1]Department of Geotechnical Engineering, Tongji University, Shanghai, China
[2]Key Laboratory for Disaster Reduction in Civil Engineering, Tongji University, Shanghai, China

Abstract

The cross-section and stiffness transition of the structure are the weak points of the seismic resistance of underground structures. In order to study the seismic response of the tunnel-group metro station in rock site, a three-dimensional finite element model of the rock-station system was established using the dynamic time-history method. Horizontal and longitudinal seismic waves were inputted, and the peak internal force response of the weak parts of the station, horizontal connecting passages, and vertical connecting passages were analysed. The results show that the stress concentration phenomenon of the station structure is related to the direction of the input seismic wave; the peak values of bending moment and axial force at the junction of the connecting passages are dominated when the earthquake transversal excitation, and the peak shear force is dominated when earthquake longitudinal excitation; the horizontal connecting passage 4 and the lower section of the vertical connecting passages are unfavourable parts of the structure under stress.

Keywords: seismic response, tunnel-group, rock site, metro station, connecting passages, peak internal force.

1 Introduction

The seismic performance of underground caverns is significantly better than that of buildings above ground due to the strong confining effect of rock medium [1]. Nonetheless, seismic damage investigations have frequently resulted in damage, destruction and even complete collapse of the underground cavern support structure

and surrounding rock. For example, after the 1999 Chi-chi earthquake, 49 of the 57 tunnels counted were damaged, and parameters such as tunnel structure layout, lining type, inverted arch setting, and lining reinforcement affect the aseismic capacity of the underground caverns [2]. And in the Wenchuan earthquake, the major damage of the mountain tunnels was mainly concentrated in the tunnel entrances, with widespread landslides and rockfalls, and the inner part of tunnels suffered moderate damages mainly due to fault displacements [3]; in the Yingxiuwan underground powerhouse, the entrance of the traffic tunnel and the exit of the tailrace tunnel were almost completely collapsed or buried by landslide, cracking and spalling were extensively observed on the reinforced concrete structures inside underground powerhouses [4]. These earthquake damages indicate that the impact of earthquakes on underground caverns needs to be further studied.

Since most analytical solutions are developed for seismic analyses of single cross-sections or regular tunnel lines [1,5], numerical modelling becomes the most frequently used method to address the seismic responses of underground caverns. Common numerical methods such as finite element method, finite difference method, discrete element method, boundary element method, etc. The outstanding advantage of the numerical method is that it can consider various practical situations such as stratum inhomogeneity, nonlinear soil-rock medium, and complex structural forms. Many scholars have studied the seismic performance of underground caverns. Wang et al. [6] established a three-dimensional dynamic finite element model to evaluate the influence of faults on the seismic performance of underground caverns; and the influence of oblique incidence of seismic waves and rock-structure interaction on underground powerhouse of the Yingxiuwan Hydropower Station. Cui et al. [7] simulated the seismic stability of the underground powerhouse of Baihetan Hydropower Station through the finite difference method. Zhang et al. [8] improved the DDA method and simulated the dynamic response of the underground powerhouse of the hydropower station. The above studies mainly focus on the underground powerhouses or underground caverns, and which are deeply buried. Special attention needs to be paid to the seismic performance of shallow underground cavities in rock site, its seismic response has not been studied extensively thus far.

In this regard, this paper takes an actual metro construction project as an example, which constructed by the drill-and-blast method. By establishing a three-dimensional finite element rock-structure system for the tunnel-group and multiple connecting passages, and inputting transversal and longitudinal seismic waves, the weak parts at the connection between the large dome station hall, vertical connecting passages, and horizontal connecting passages are studied in detail, including the stress distribution characteristics and force situation at the connection.

2 Prototype Problem

This article is based on a metro station in Qingdao, China. The station adopts a structure with separate hall and platform areas as well as separate left and right platforms. The main tunnel length of the hall is 183.2 m, while length of the platform area is 169.1 m. The double-layered arched top of the hall is buried 15 m deep, and

multiple horizontal and vertical passages connect the hall and platform, forming a three-dimensional spatial structure. This type of metro station is the first kind in China. Figure 1 shows a sectional view of the station, where passengers can shuttle between the hall and platform via vertical connecting passages, and transfer between different lines through horizontal connecting passages. Air ducts connect the hall and platform for ventilation purposes.

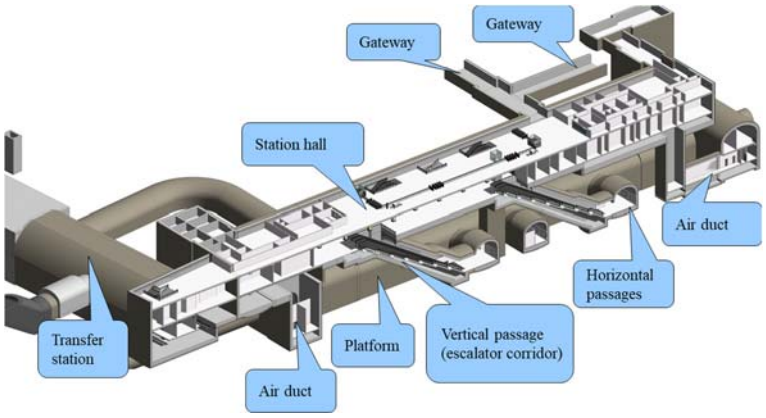

Figure 1: Schematic diagram of station structure section.

The arch-cover method was used to construct the tunnel in the station hall, while the step method was used for excavation in the platform. Due to the complex structure, numerical simulation is needed to calculate the seismic performance of the structure. To simplify the modelling process, the air ducts were simplified into horizontal connecting passages. The simplified side view of the metro station structure is shown in Figure 2, which consists of five horizontal connecting passages and two vertical connecting passages. The specific dimensions of the horizontal and vertical connecting passages are shown in Figure 3.

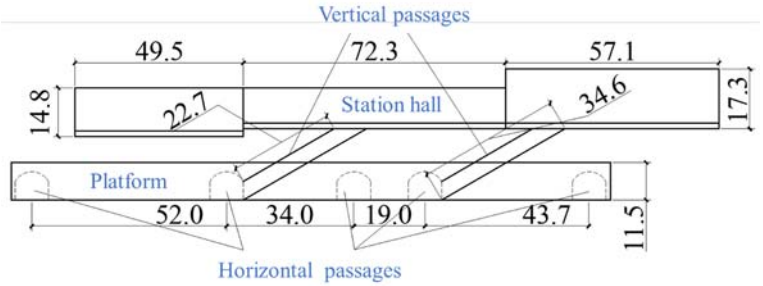

Figure 2: Side view of station structure (unit: m).

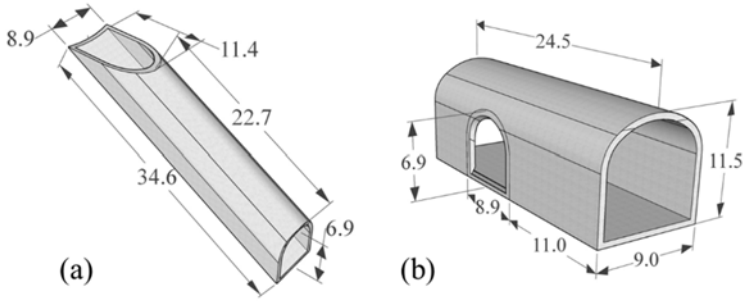

Figure 3: Schematic diagram of the connecting passages: (a) vertical passage; (b) horizontal passage (unit: m).

3 Dynamic Analysis Model

3.1 Finite Element Model

This article used the ABAQUS software to establish a 3D finite element model to analyse the seismic response of a group-tunnel metro station. According to the Seismic Design Code [9] and research by Y. Yuan et al. [10], the model has a planar size of 300 meters (in the transverse direction) × 400 meters (in the longitudinal direction) × 70 meters (in the depth direction), meeting the requirement that the distance from the boundary is greater than three times the width of the structure. The cross-section of the numerical model is shown in Figure 4. The surrounding rock adopts solid element C3D8R, and the lining adopts shell element S4R. The number of grids is about 100,000, and the maximum grid size near the structure is 5 meters, which is less than 1/8 of the wavelength corresponding to the maximum frequency of the wave [11]. The grid division follows the principle of densification near the structure. The lateral artificial boundary of the model adopts an equivalent displacement boundary, that is, binding the degrees of freedom of corresponding points at equal heights on the boundary in the direction of inputting seismic wave, while relaxing the degrees of freedom in other directions.

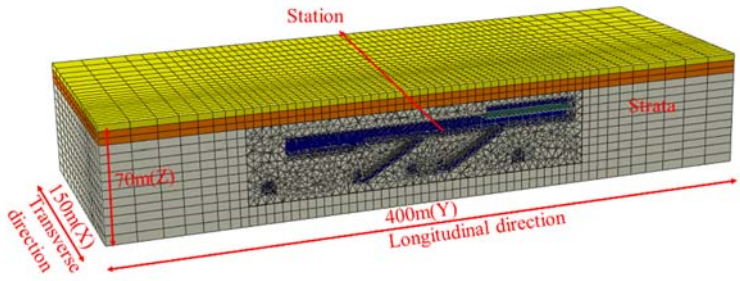

Figure 4: Sectional view of 3D finite element model (unit: m).

3.2 Model Parameters

In numerical simulations, in order to simplify the calculations, the station structure is treated as a homogeneous and continuous concrete material using a linear elastic

model for simulation. For the station structure, C45 concrete is used for the central column and central plate, while C30 concrete is used for all other parts, and the material parameters are determined according to the "Code for Design of Concrete Structures" (GB 50010-2010). And the tunnel structure is connected to the surrounding rock using TIE connections. The calculation material parameters for the tunnel structure are shown in Table 1.

Concrete grade	Elastic modulus (GPa)	Density (kg/m^3)	Poisson's ratio
C30	30	2500	0.2
C45	33.5	2550	0.2

Table 1: Physical parameters of lining structure.

Simplified treatment can be applied to the stratum, according to the "Engineering Rock Mass Classification Standard" (GB/T 50218-2014), in which moderately weathered granite is classified as a Grade III rock mass and highly weathered granite is classified as a Grade IV rock mass. The stratum adopts the Mohr-Coulomb yield criterion. Table 2 lists the physical and mechanical properties of the stratum.

Stratum	Thickness (m)	Weight (kN/m^3)	E (GPa)	Friction angle (°)	Cohesion (MPa)	Poisson's ratio
Fill soil	2	21	0.2	16	0.05	0.45
Strong weathered granite	8	23	3	30	0.6	0.32
Moderately weathered granite	60	25.5	11	36	1.1	0.28

Table 2: Physical parameters of stratum.

Site damping is calculated using Rayleigh damping. The formulas are shown in Equation (1) and (2).

$$C = \alpha M + \beta K \tag{1}$$

$$\begin{Bmatrix} \alpha \\ \beta \end{Bmatrix} = \frac{2\omega_i\omega_j}{\omega_i^2 - \omega_j^2} \begin{bmatrix} \omega_j & -\omega_i \\ -\frac{1}{\omega_j} & \frac{1}{\omega_j} \end{bmatrix} \begin{Bmatrix} \zeta_i \\ \zeta_j \end{Bmatrix} \tag{2}$$

Among them, α, β is the mass and stiffness coefficient; ω_i, ω_j corresponding to two target frequencies, respectively; ζ_i, ζ_j is the modal damping ratio of the covering stratum; generally, it is often assumed $\zeta_i = \zeta_j = \zeta$ and taken as 0.05. After simplification, it is shown in Equation (3).

$$\begin{Bmatrix} \alpha \\ \beta \end{Bmatrix} = \frac{2\zeta}{\omega_i + \omega_j} \begin{Bmatrix} \omega_i\omega_j \\ 1 \end{Bmatrix} \tag{3}$$

3.3 Seismic Cases

When using the dynamic time history method to analyse the dynamic response of the structure, consider the fortification earthquake effect. The input motion was loaded in two different directions: the transversal direction (excitation direction perpendicular to the tunnel axis) and longitudinal direction (excitation direction parallel to the tunnel axis). The designed peak ground acceleration is 0.1g, and the acceleration time history and spectrum curve of the earthquake wave after amplitude and baseline correction are shown in Figure 5. Before the dynamic calculation, the initial stress balance of the system is firstly carried out.

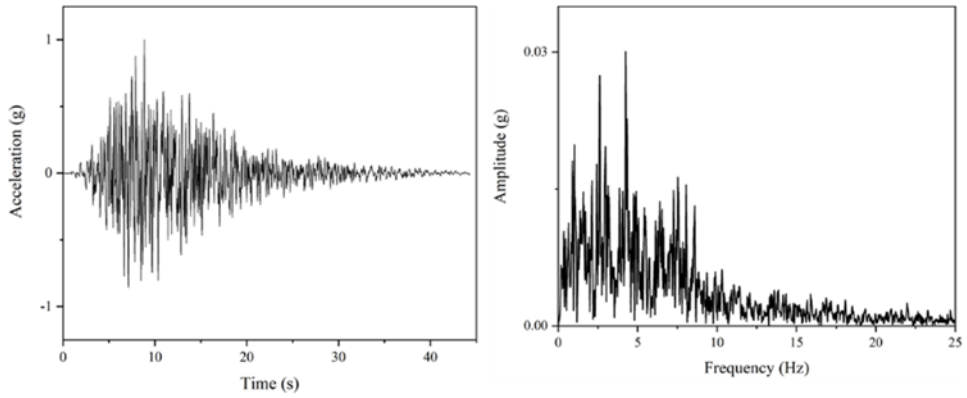

Figure 5: Artificial wave acceleration time history and spectrum curve.

4 Results and Discussion

4.1 Weaknesses of the Structure

Due to the complex spatial structure of the tunnel-group metro station, the stiffness of the structure is large in the hall and platform, while the vertical and horizontal connecting passages have smaller stiffness. Therefore, there is a problem of cross-sectional and stiffness transitions, and special attention should be paid to the safety and reliability of their connections. As shown in Figure 6, the maximum principal stress distribution of the connecting passages under transverse and longitudinal seismic waves. It is observed that stress concentration occurs at the arch shoulder of the connection between the vertical and horizontal connecting passages when transversal excitation; stress concentration occurs at the arch bottom of the connection between the horizontal connecting passage and the platform when longitudinal excitation. This is because under the action of seismic motion, relative displacement occurs between different parts of the structure, causing large tensile stresses at the structural connections, which may cause concrete cracking or even further damage, and need special attention.

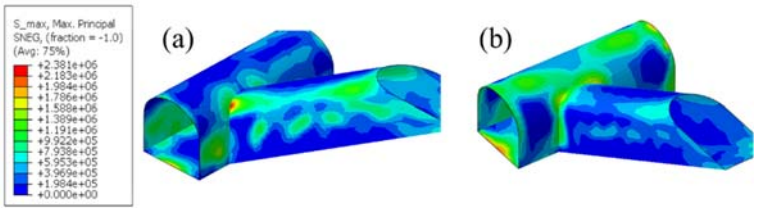

Figure 6: Maximum principal stress distribution of the structure under earthquake excitation: (a) transverse direction; (b) longitudinal direction.

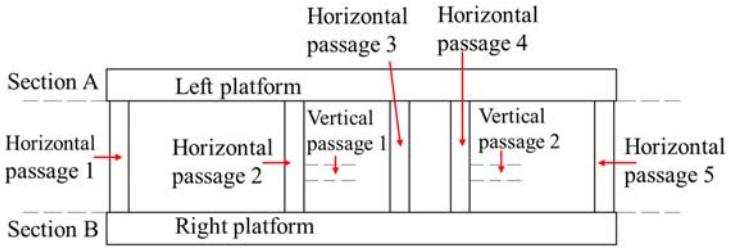

Figure 7: Schematic diagram of the connecting passages

4.2 Dynamic Response of Horizontal Connecting Passages

Figure 7 is a plan view of the connecting passages, and sections A and B are the connection points between the horizontal connecting passages and the platforms. The five horizontal connecting passages are numbered 1 to 5 from left to right. Figure 8 shows the local coordinate system directions of the internal forces in the structure. The dynamic response of the structure mainly focuses on the bending moment, axial force, and shear force at the connection points, corresponding to the bending moment and axial force along axis 1 and the shear force along axis 2 in Figure 8. The analysis of the dynamic response of the vertical connecting passages is similar to that of the horizontal connecting passages, focusing on the internal force at the connection point between the upper and lower sections.

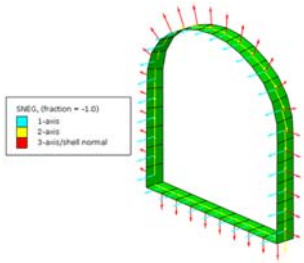

Figure 8: Schematic diagram of the local coordinate system of the structural internal force

The changes in peak internal forces in the horizontal connection passages at sections A and B are shown in Figure 9. When earthquake transversal excitation, the maximum bending moment is at passage 4, and the bending moment values at the junctions of passages 1, 2, and 5 are relatively close. The maximum shear force occurs

at section B of passage 3; the maximum axial force occurs at section A of passage 4. When earthquake longitudinal excitation, the maximum bending moment occurs at passage 3; the maximum shear force occurs at section A of passage 4; the maximum axial force occurs at section A of passage 4. Overall, the bending and axial force peak at the junctions of the connecting passages dominate when transversal excitation, and the shear force peak dominates when longitudinal excitation. The connection point of connecting passage 4 is the more unfavourable part of the structure.

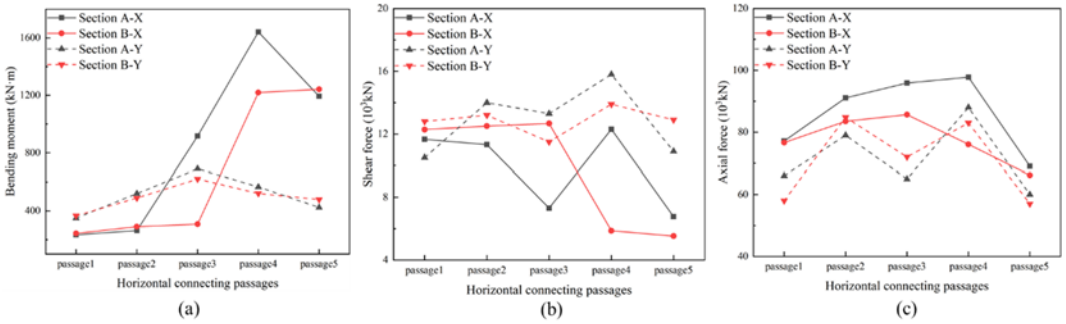

Figure 9: The peak internal force at the connection of the horizontal connecting passages: (a) bending moment; (b) shear force; (c) axial force.

4.3 Dynamic Response of Vertical Connecting Passages

Similarly, the peak internal forces in the upper and lower section of the vertical connecting passages were analysed, as shown in Figure 10. Through data analysis, it was found that the peak internal forces in the upper section were always smaller than those in the lower section. In general, the peak bending moment and axial force dominate during transversal excitation, while the peak shear force dominates during longitudinal excitation. Therefore, the connecting part of the lower section in the vertical connecting passage is the more unfavourable part for stress.

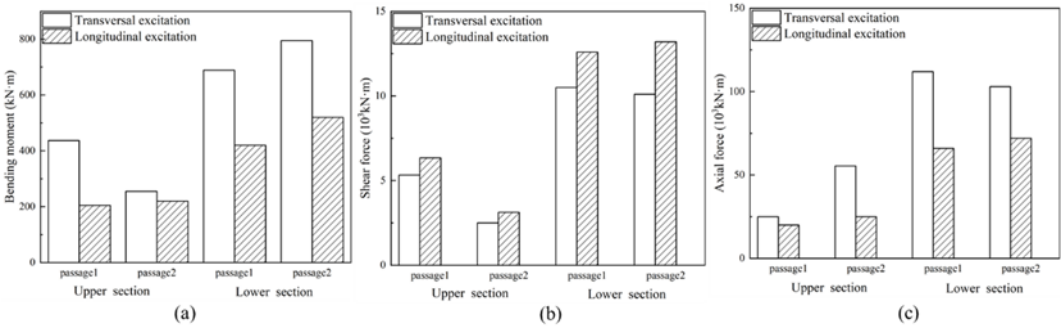

Figure 10: The peak internal force at the connection of the vertical connecting passages: (a) bending moment; (b) shear force; (c) axial force.

5 Conclusions

This paper established a detailed 3D finite element model of a tunnel-group metro station in rock site and used dynamic time-history analysis to study the seismic

response of this special structure form, focusing on the weak points at the connection between the connecting passages and the tunnels. The following conclusions can be drawn:

(1) When the earthquake excitation direction changes, stress concentration phenomena of the station structure will occur in different parts, which is the seismic weak point of the connection.

(2) The bending moment and axial force peak values at the horizontal connecting passage dominate when earthquake transversal excitation, while the shear force peak value dominates when earthquake longitudinal excitation. The horizontal connecting passage 4 is an unfavourable location for stress, which may cause concrete cracking or even further damage.

(3) The bending moment and axial force peak values at the vertical connecting passage dominate when earthquake transversal excitation, while the shear force peak value dominates when earthquake longitudinal excitation. The lower section of the vertical connecting passage is an unfavourable location and should be focused on seismic design.

Acknowledgements

The authors gratitude the financial support from National Natural Science Foundation of China (51478343 & 51778487& 52061135112).

References

[1] Y. M. Hashash, J. J. Hook, B. Schmidt, I. John, C. Yao, “Seismic design and analysis of underground structures”, Tunnelling and underground space technology, 16(4), 247-293, 2001.

[2] W. L. Wang, T. T. Wang, J. J. Su, C. H. Lin, C. R. Seng, T. H. Huang, “Assessment of damage in mountain tunnels due to the Taiwan Chi-Chi earthquake”, Tunnelling and underground space technology, 16(3), 133-150, 2001.

[3] Z. Wang, B. Gao, Y. Jiang, S. Yuan, “Investigation and assessment on mountain tunnels and geotechnical damage after the Wenchuan earthquake”, Science in China Series E: Technological Sciences, 52, 546-558, 2009.

[4] X. Wang, J. Chen, M. Xiao, “Seismic damage assessment and mechanism analysis of underground powerhouse of the Yingxiuwan Hydropower Station under the Wenchuan earthquake”, Soil Dynamics and Earthquake Engineering, 113, 112-123, 2018.

[5] C.M. St John, T. F. Zahrah, “Aseismic design of underground structures”, Tunnelling and underground space technology, 2(2), 165-197, 1987.

[6] X. Wang, J. Chen, M. Xiao, “Seismic damage assessment and mechanism analysis of underground powerhouse of the Yingxiuwan Hydropower Station under the Wenchuan earthquake”, Soil Dynamics and Earthquake Engineering, 113, 112-123, 2018.

[7] Z. Cui, Q. Sheng, X. Leng, “Effects of a controlling geological discontinuity on the seismic stability of an underground cavern subjected to near-fault ground motions”, Bulletin of Engineering Geology and the Environment, 77, 265-282, 2018.
[8] Y. Zhang, X. Fu, Q. Sheng, “Modification of the discontinuous deformation analysis method and its application to seismic response analysis of large underground caverns”, Tunnelling and Underground Space Technology, 40, 241-250, 2014.
[9] Ministry of Housing and Urban-Rural Development of the People's Republic of China, “Code for seismic design of urban rail transit structures: GB50909-2014”, Beijing: China Planning Press, 2014.
[10] Y. Yuan, Q. Wang, X. Cai, “Analysis of Lateral Seismic Response of Road Tunnel Structure in Deep Soft Soil Area”, China Municipal Engineering, 79-83+119, 2020.
[11] R. L. Kuhlemeyer, J. Lysmer, “Finite element method accuracy for wave propagation problems”, Journal of the Soil Mechanics and Foundations Division, 99(5), 421-427, 1973.